QinetiQ

Deep-Space Optical Communication Compatible Multifunction LIDAR

Executive Summary Report

Author David Orchard

Document Ref: QINETIQ/EMEA/CIT/1801759
Issue: 1.0
Date: 12th September 2018
Total pages: 12

Requests for wider use or release must be sought from:

Simon Bray
Building CB, Room A233
QinetiQ Limited
St Andrews Road
Malvern
WR14 3PS
United Kingdom

Administration page

Customer Information	
Project title	DEEP-SPACE OPTICAL COMMTINICATION COMPATIBLE MULTIFUNCTION LIDAR
Document title	Executive Summary Report
Customer organisation	ESA
Customer contact	Clemens Heese
Contract number	4000118330/16/NL/BJ

Authors	
Name	
David Orchard	
Responsibility	Date 12th September 2018
Project team members	

Product Assurance Approved By	
Name	
Dr Chris West	
Responsibility	Date 12th September 2018
Independent Reviewer	

Approved By	
Name	
Simon Bray	
Responsibility	Date 12th September 2018
Project Manager	

Record of changes

Issue	Date	Detail of Changes
0.1	24/08/2018	First draft
1.0	12/09/2018	Issued

Table of Contents

1 Introduction

This document is the Summary Report for the programme “Deep Space Optical Communication Compatible Multifunction Lidar”.

1.1 Background

Optical communication terminals have many subsystems in common with lidar systems for optical range measurements and 3D surface mapping. For example, both systems require a seed laser, a means for modulating some property of the light (amplitude, frequency, phase or some combination), optical amplifiers and free-space beam forming optics. Provision is also made for coarse and fine pointing in most cases. By adding a detector subsystem to measure returning light from reflections, and with some additional modification to the software, an optical communications architecture can be extended to a lidar system.

This is especially attractive as a communications payload does not acquire scientific data, but is considered part of the spacecraft platform. Due to orbital dynamics constraints, the duration of an optical communications link to Earth is often limited. This leaves time to use the payload for other operations, i.e. ranging or 3D surface mapping of an asteroid. The data can be stored in the optical communications buffer and downloaded as soon as Earth line-of-sight is available.

With this dual mode operation, one can make maximum use of the weight investment in an optical communications payload. Combining a LIDAR with a high-speed optical terminal also appears to be a natural match. One part is able to generate a high data volume (point cloud data on 3D surface) and the other part is able to provide the bandwidth to relay the data back to Earth.

A study has been conducted into the feasibility of upgrading an optical communications terminal to add lidar functionality. The model for the deep-space communications terminal was the OPTEL-D payload developed for the ESA AIM mission. A lidar concept was developed to make maximum re-use of the OPTEL-D hardware and a breadboard was constructed to test the concept. The results have been compared with a numerical model of the system.

2 Lidar design

2.1 Functional diagram

A functional diagram of the design is shown in Figure 2-1. The design can be divided into four main elements: fibre optical source, free space optics and beam director, detection sub-system, and control and data processing system. With the exception of the detection sub-system, much of the necessary hardware is present in OPTEL-D.

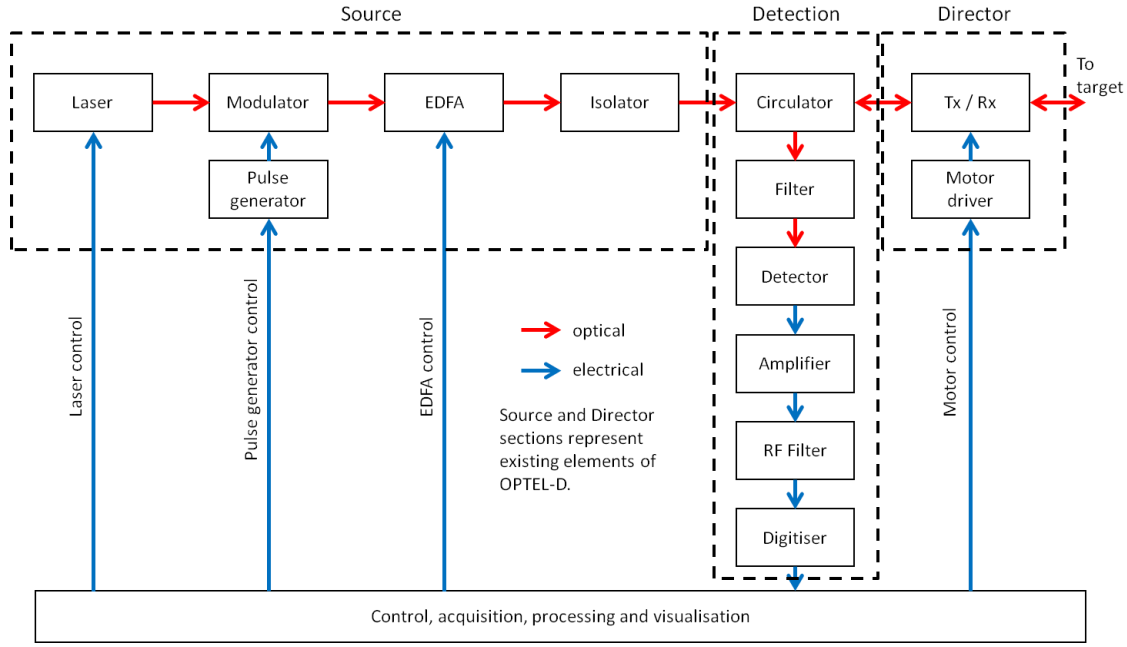

Figure 2-1: Block diagram of breadboard lidar

A number of options were considered for the receiver path, including completely independent optics for the transmitter and receiver. The option shown in Figure 2-1, to introduce a circulator in the transmit path, makes the most efficient use of the existing optical aperture for both transmit and receive with minimal change to the OPTEL-D optical design. High power circulators from two different manufacturers were tested and found to be robust to continuous pulsed operation at peak powers of 1.2 kW and average powers of 3 W.

2.2 Modulation scheme

A novel element of the lidar design is the modulation scheme that allows the use of pseudo-random binary sequences (PRBS) with the OPTEL-D architecture by exploiting the pulse-position modulation (PPM) encoding scheme used by the communications mode of OPTEL-D.

If 1s and 0s were encoded respectively by the presence or absence of a laser pulse, the long sequences of 0s found in a high-order PRBS sequence would allow the build-up of a large population inversion in the EDFA. If this were subsequently released in a single giant optical pulse, there would be a significant risk of damage to the optical system. An alternative encoding scheme was therefore developed, in which '1s' and '0s' in a PRBS sequence were encoded by pulses in two of the PPM time-slots. A pulse would be transmitted in every frame and there would be no long periods without a pulse being transmitted. Effectively, two complementary sequences are transmitted, slightly displaced in time. When correlated with the corresponding template, the correlation pattern contains a single large positive peak of amplitude M, two adjacent negative peaks of amplitude M/2 and small sidelobes of amplitude ±1 at regular intervals throughout, where M is the length of the sequence, typically 1023.

To make a measurement, the sequence of pulses was transmitted repeatedly and the returns from a remote target were accumulated into a buffer. After correlation, the location of the

strongest pulse provides the range to the first target (typically the lidar optics themselves). The pulse and its corresponding sidelobes can then be subtracted to reveal the signals from weaker targets. This scheme allows the detection of signals over a wide dynamic range (>10^5).

2.3 Breadboard

A breadboard lidar system (Figure 2-2) was designed and manufactured based on the concept described in section 2.1. The breadboard system was designed to emulate as far as possible the relevant characteristics of the OPTEL-D system using COTS components.

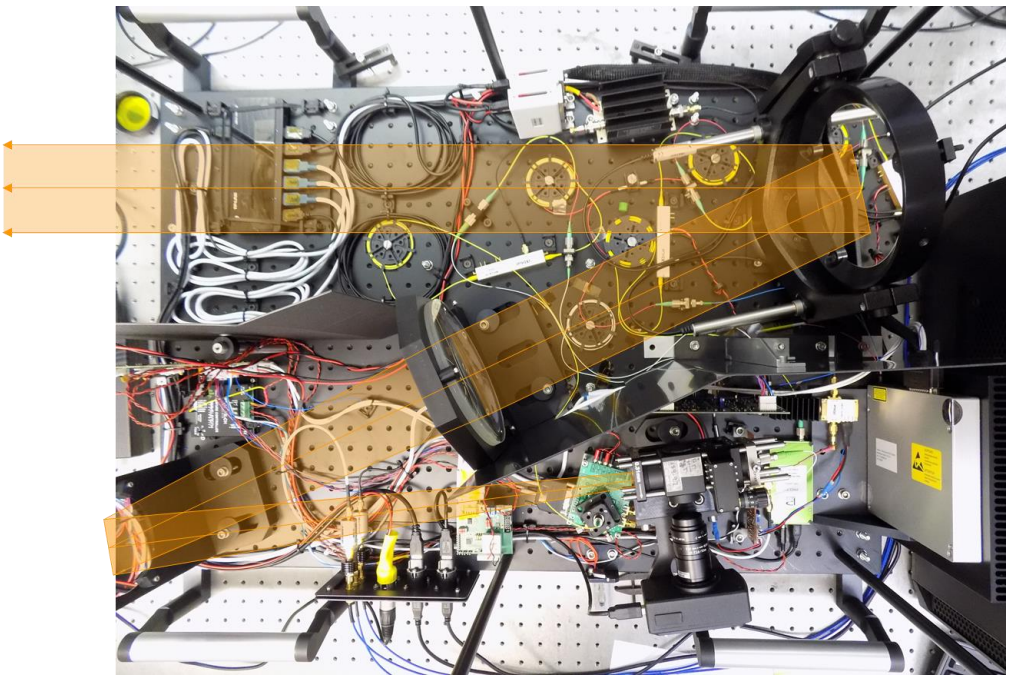

Figure 2-2: Plan view of optical head with beam path superimposed

The optical source was a standard telecoms laser, followed by an electro-optic modulator and EDFA. The peak pulse power obtained from the system was limited in early experiments by the contrast ratio of the modulator, with much of the EDFA output power remaining unmodulated. When the modulator was replaced with a high-contrast variant, a greater fraction of the output power was contained in the pulses, which allowed the EDFA to be operated at lower average output powers for the same peak power. The maximum output power was limited by Stimulated Brillouin Scattering (SBS), which was observed at high peak powers. This was found to be detrimental to the lidar performance and so the source was typically operated at modest peak powers of ~150W during lidar tests, with a pulse repetition frequency of 200 kHz.

The detector was an InGaAs avalanche photodiode (APD). A modulator was used to minimise the light reaching the APD to coincide with the internal reflections. This was found to improve the sensitivity of the lidar to weak reflections from remote targets.

The breadboard is controlled by a PC, which houses the 300 MHz digital-to-analogue converters (DAC) for generation of the modulator signals and the 150 MHz analogue-to-digital converter (ADC) for digitisation of the APD output. The DACs and the ADC are integrated on a single electronics board and are synchronised to a common clock. A GPS-based clock was used to provide a high accuracy reference frequency and hence accurate range measurements.

The software for the breadboard has been written in Python and controls all aspects of the system. All data from each measurement are saved to file for subsequent processing.

3 Test campaign

A test campaign was conducted to measure the performance of the lidar under a range of conditions. The lidar was tested at ranges from less than 100 m to 17.7 km.

3.1 Measurement conditions

The lidar was installed in a laboratory at QinetiQ Malvern with views across the Severn Vale. A calibrated diffuse target was installed in a field 7.6 km from the laboratory. Measurements were made to both the calibrated target and to other features such as buildings within the field of view.

Measurements were of 1 second duration using a pulse repetition frequency of 200 kHz and a peak power of ~150 W. The pulse width was 10 ns FWHM. Measurements were made under a variety of atmospheric conditions varying from bright sunshine to overcast to light drizzle. The maximum range under which measurements could be made to diffuse targets was limited to ~8 km by atmospheric turbulence. Measurements to a small corner cube target were readily achieved at 17.7 km.

3.2 Measurements to diffuse targets

Measurements of the range to diffuse targets were made at distances from 10s of metres to 7.6 km. Measurements at longer range were hampered by atmospheric turbulence, which caused beam break-up and beam wander and hence loss of signal at the receiver. The standard deviation of the measurements at short range was typically 0.06 m. At the maximum range, the standard deviation was slightly larger, 0.087 m, due to turbulence. Measurement accuracy was apparently unaffected by movements of 0.5 ms^{-1}, both along and transverse to the line of sight, the range returned being the average position of the target during the measurement period. The lidar was able to track range changes along the line of sight at an update rate of 10 Hz.

Scans were made of a number of targets to demonstrate the capability to resolve surface structure. *Figure 3-1* shows a scan of a building approximately 7.2 km from the laboratory. The scan reveals details of the surface profile of the building, including the curved frontage and the recessed regions at the side.

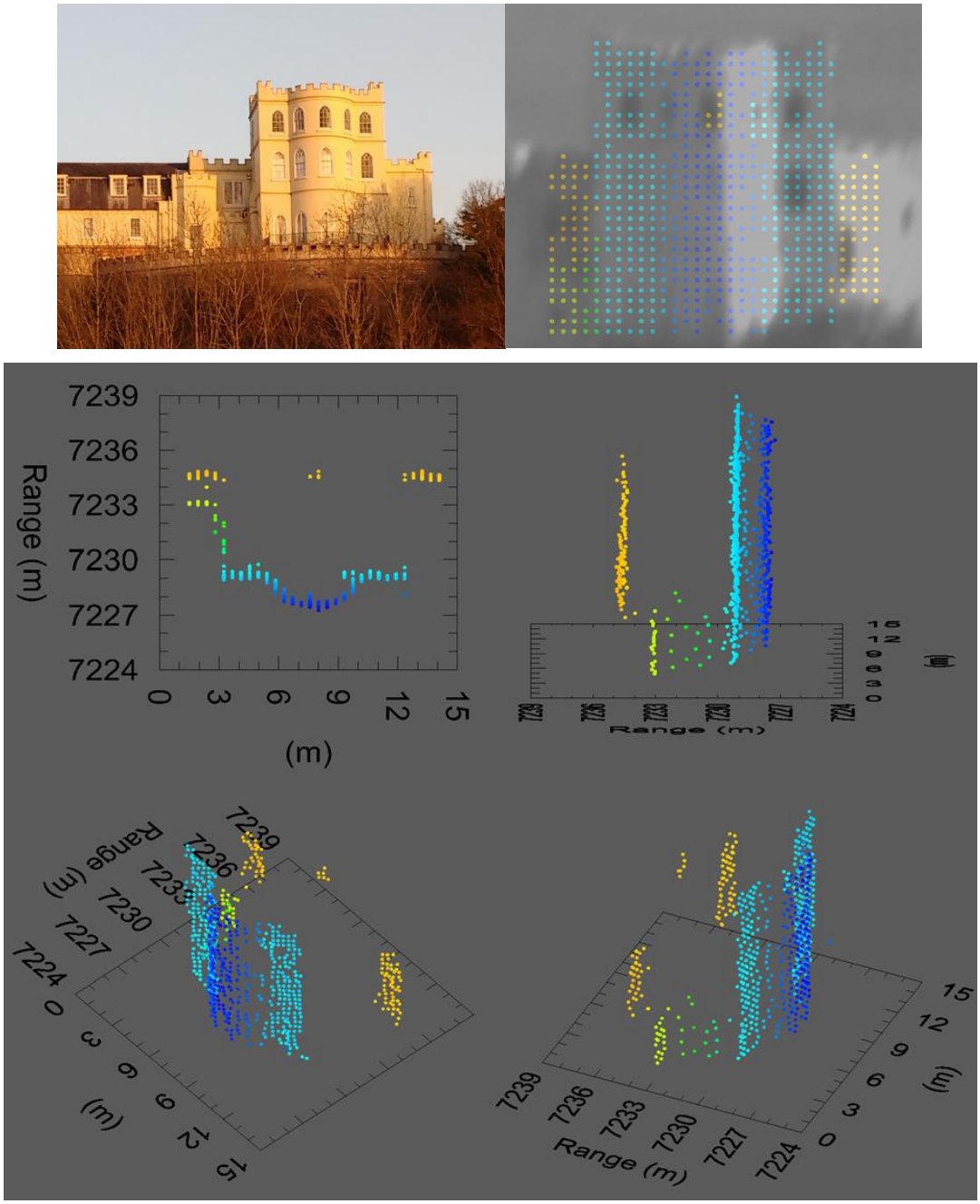

Figure 3-1: Scan of Severn Bank House. Top: Image of Severn Bank House (left); View from the lidar camera with overlaid scan points (right). Bottom: 3-D views of the scan from different angles.

3.3 Verification of range-finder accuracy

A small corner cube was used as a point-like target to verify the accuracy of the lidar over extended ranges. Range measurements to the corner cube were made at a selection of distances from a few 100s of metres to 17.7 km. The position of the corner cube at each location was determined using a high-precision GPS surveying system. After correction for the refractive index of air, the regression fit between the surveyed and measured ranges was linear with a slope of unity. All lidar measurements were within 0.4 m of the survey results.

3.4 Performance against programme goals

Table 1 shows a summary of the performance of the lidar breadboard. In most cases the performance of the breadboard has been verified as meeting the programme goal. In some cases it has been possible only to partially verify the performance against the goal due to

limitations of the test environment. Extrapolation of the breadboard performance to a more benign environment (i.e. vacuum) suggests that most of the goals could be achieved, although it may not be feasible to measure to low reflectivity targets at the maximum range.

Parameter	Goal	Verified	Achievable
Minimum range	100 m	Yes	Yes
Maximum range	35 km	In Part[1]	In Part[2]
Range precision (3σ)	0.2 m	Yes	Yes
Range trueness	0.5 m	Yes	Yes
Surface resolution	0.3 m	In Part[3]	Yes
Relative motion	0.5 ms^{-1}	Yes	Yes
Measurement rate	1 Hz	No[4]	Yes

Table 1: Summary of breadboard performance

Notes:

1. *Maximum accessible range at the test site was limited to ~18 km.*
2. *Analysis of test results and extrapolation to a vacuum environment indicate that high albedo targets could be detected at a range of 35 km.*
3. *The resolution during testing was limited by beam spreading and beam wander caused by atmospheric turbulence.*
4. *The data acquisition rate of the breadboard was sufficient to achieve the 1 Hz goal, but the calculation of the range was limited by the speed of the computer processor. A measurement rate of 1 Hz or better could be achieved in a future development of the system by using an FPGA-based processor.*

3.5 Factors affecting performance

The limiting factor in the capability of the lidar to make measurements under various scenarios is the signal to noise ratio (SNR). The effective SNR of the breadboard was lower than predicted due to excess detector noise and clutter arising from the strong narcissus reflection.

The performance of the lidar could be improved either by reducing the magnitude of the narcissus signal or by reducing the sensitivity of the detector to the narcissus signal. It is unlikely that the narcissus could be significantly reduced, without resorting to a complete separation of the transmitter and receiver, which would significantly increase the complexity of the design. However, the sensitivity of the detector to the narcissus could be minimised by improved circuit design. Such an approach merits further investigation during future development of this technology.

4 Numerical model

4.1 Overview

A numerical model has been written to simulate the performance of the lidar. The model was written in a high level language (Python v3.6).

The model simulates the operation of the lidar from transmission of the probe beam to analysis of the receiver signal. The model includes the following features:

- Multiple moving targets;
- Configurable modulation of probe beam;
- Optical propagation of probe beam from transmitter to receiver;
- Detailed modelling of the detection process including noise;
- Analysis of digitiser signals to produce target information (range, signal strength).

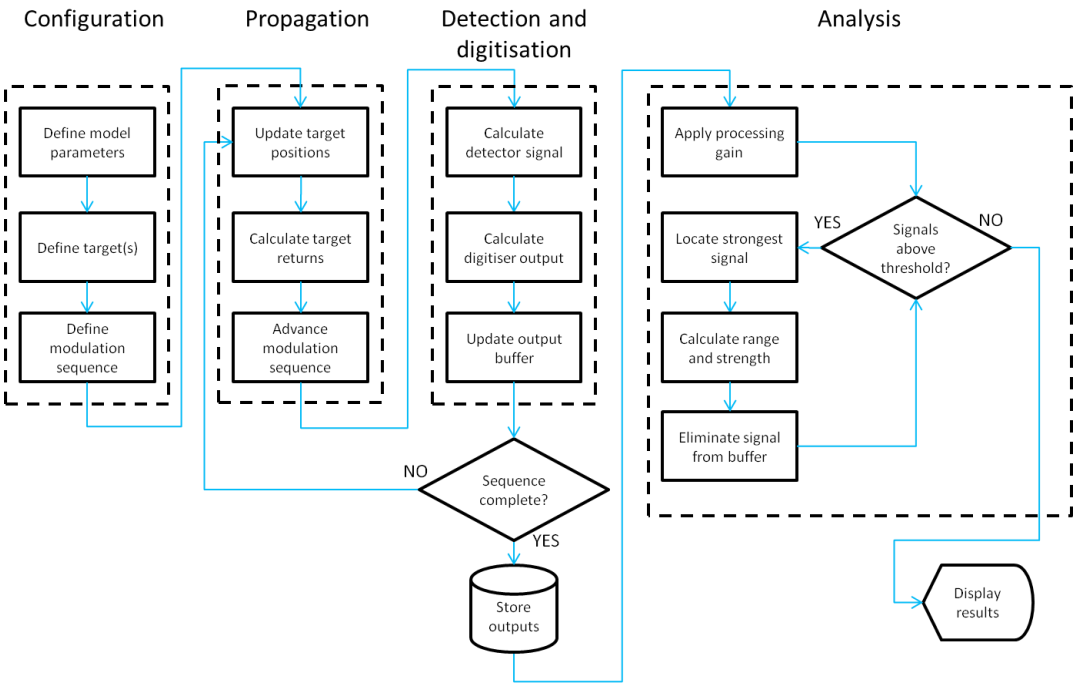

Figure 4-1: Simulation flow diagram

Figure 4-1 shows a flow diagram of the simulation. Once the simulation has been configured, the signals are calculated for a portion of the measurement sequence. The target positions are then updated and the calculations are repeated for the next portion of the sequence, accumulating the results in a buffer until the sequence is complete and the return from the last part of the sequence from the farthest target has been received. The results are then stored and analysed to calculate the range.

4.2 Verification and validation

The model was verified by comparing results for a number of simple scenarios against *a priori* calculations. *Figure 4-2* shows the coupling efficiency from source to detector as a function of range to the target. The efficiency follows an inverse-square law at long ranges, but is nearly constant at short ranges, because the light is collected by a single-mode fibre. This is a key result for the lidar as it significantly reduces the dynamic range required of the detector.

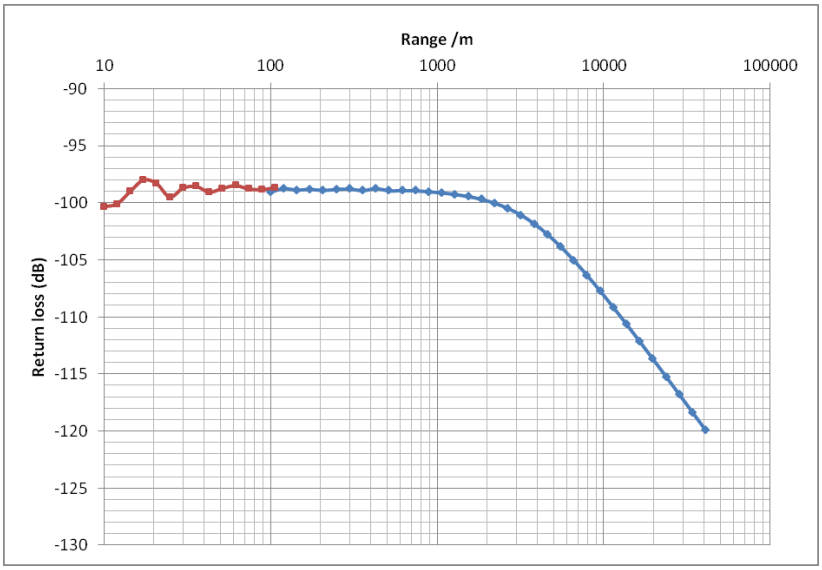

Figure 4-2: Coupling efficiency from the output beam via a plane diffuse target to a single mode fibre as a function of range.

The model was used to simulate the output of the lidar breadboard for a number of scenarios representative of measurements made during the test campaign.

Table 4-1: Comparison between measured and simulated data at 7.6 km.

Range = 7.6 km	**Simulated**	**Experimental**
Signal counts	2.8×10^6	$0.8 \times 10^6 – 3.6 \times 10^6$
Threshold counts (5σ)	2.1×10^5	~8×10^5
SNR	~65	5 – 22
Range standard deviation (m)	0.016	0.089

NB The table includes only experimental results above the detection threshold.

Table 4-2: Comparison between measured and simulated data at 96 m.

Range = 96 m	**Simulated**	**Experimental**
Signal counts	7.6×10^7	$2.5 \times 10^7 – 9.5 \times 10^7$
Threshold counts (5σ)	2.2×10^5	~8.8×10^5
SNR	~1730	142 – 540
Range standard deviation (m)	0.0005	0.061

Table 4-1 and *Table 4-2* show a comparison between experimental and simulated measurements. The threshold is the signal level required for detection, derived from the noise.

Overall, the simulation provides a good model for the propagation and detection of the light reflected from the target, but significantly underestimates the noise level. This is because the strong narcissus reflection caused excess noise in the detector, which is not included in the simulation.

5 Conclusions

The feasibility of adding lidar functionality to a deep-space optical communications terminal has been demonstrated.

A breadboard lidar has been designed and constructed based on the specifications of the OPTEL-D terminal. Tests have demonstrated useful lidar performance at ranges up to 7.6 km in a turbulent atmosphere. Extrapolation of the results indicate that range measurements to diffuse targets in a vacuum should be possible a ranges of up to a few tens of kilometres.

A numerical model has been developed to support the development of the breadboard. The model produces estimates of signal strength and noise based on the parameters of the system components. The model performs at low signal levels. A revised detector model is required to accurately predict the excess noise generated from strong optical signals.

A space-grade version of the system could be developed in a fairly short timescale. Key activities would be the qualification of the circulator for the space environment and implementation of the lidar algorithms on an FPGA-based platform. The sensitivity of the system would benefit from improvements in detector technology and circuitry to reduce the impact of strong reflections from the internal optics.